Code Properties Analysis for the Implementation of a Modulated Wideband Converter

Marguerite Marnat*, Michaël Pelissier*, Olivier Michel† and Laurent Ros†
*Univ. Grenoble Alpes, F-38000 Grenoble, France
CEA, LETI, MINATEC Campus, F-38054 Grenoble, France
†GIPSA-Lab, Image and Signal Department, F-38402 Saint-Martin-d'Hères, France
Email: marguerite.marnat@cea.fr, michael.pelissier@cea.fr

***Abstract*—This paper deals with the sub-Nyquist sampling of analog multiband signals. The Modulated Wideband Converter (MWC) is a promising compressive sensing architecture, foreseen to be able to break the usual compromise between bandwidth, noise figure and energy consumption of Analog-to-Digital Converters. The pseudorandom code sequences yielding the sensing matrix are yet the bottleneck of it. Our contributions are multifold: first, a proposal of a new Zadoff-Chu code based real-valued sensing matrix that satisfies cyclic properties and good spectral properties and increases robustness against noise. Second, a quasi systematic study of the influence of code families and of row selection is carried out on different criteria. Especially, the influence on the coherence, vital to limit the number of branches, is investigated. Additionally, an original approach that focuses on evaluating isometric properties is established. These measures are helpful since isometry is essential to noise robustness. Third, the relevance of previous high-level metrics is validated on various codes thanks to a simulation platform. Altogether this study delivers a methodology for a thorough comparison between usual compressive sensing matrices and new proposals.**

I. Introduction

A. The Modulated Wideband Converter (MWC)

Compressive sensing is a paradigm shift introduced in 2006 by [1] which goes beyond the Nyquist criteria. Given that there is a basis in which few coefficients suffice to represent the signal, the idea is to measure just the essential information instead of acquiring redundancies at Nyquist rate. Recovery is made possible by this sparsity assumption if we succeed in creating enough diversity between the measures. Random demodulators are among the most popular "Analog-to-Information Converters" to date and in particular the Modulated Wideband Converter (MWC) introduced by Mishali [2]. As can be seen on Fig. 1 the principle of a MWC is to multiply the K-sparse (K active frequency subbands) input signal in each of the M parallel branches with functions based on codes. For each branch $i \in \{1, ..., M\}$, the mixing function $p_i(t)$ is T_p-periodic and consists, within each period, in a code $\mathbf{c}_{i,.}$ of N elements, shaped with rectangular chip pulses. MWC parameters verify $N.f_p = 2.f_{max}$ where f_{max} is the upper bound of the analyzed frequency span and $f_p = 1/T_p$. The spectrum is thus convolved with a f_p-spaced Dirac comb so that each band is weighted by the corresponding Fourier coefficient of the code and the whole spectrum is aliased at baseband. The last step consists in low-pass filtering ($h(t)$

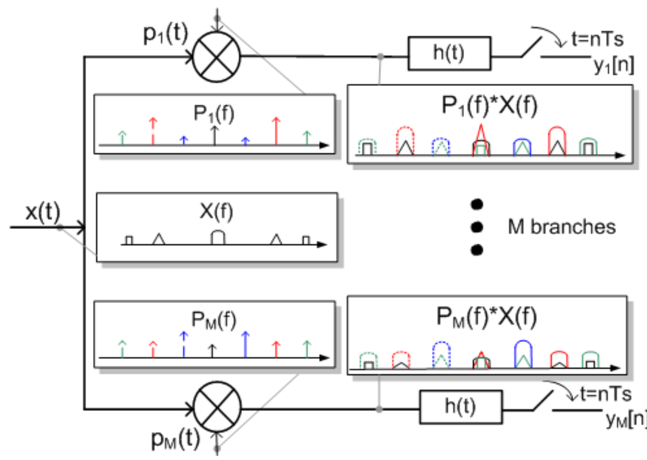

Fig. 1: Sensing process of the MWC.

on Fig. 1) with cut-off frequency $f_c = 1/2.T_s$ and uniform sampling at f_s (by default $f_s = 1/T_s = f_p$).

Codes are crucial as they give the coefficients of the output mixture. Up to our knowledge, selecting a code from a set of required properties has not yet been studied methodologically in an exhaustive way. In this paper, some key properties serve as a cornerstone for selecting suitable codes: orthogonality, correlations and norm preservation. The interest of our study lies in proposing evaluation criteria, illustrated through examples and simulations.

B. State-of-the-art of the mixing codes

Most publications ([1],[3],[4]) stay on the theoretical level and use random codes, generated by independent and identically distributed (i.i.d.) processes with e.g. Gaussian or Bernoulli probability density function. Typically, following codes are implemented: a random Bernoulli operator [2] requiring $M.N$ flip-flops or Gold sequences [5] with N of the form $2^n - 1$ (n $\in \mathbb{N}$). Circulant matrices generated in the frequency domain from a maximal or Legendre sequence also promise some benefits [6] but require complex implementation.

Because they run at the Nyquist rate, those codes represent most of the energy consumption of the MWC [7]. Another imperative is the limitation of the number of branches M in order to minimize consumption and die area. But fewer

ISBN 978-0-9928626-7-1 © EURASIP 2017

measurements means that if the code has bad properties (see Sect. II-A on coherence), the highest sparsity degree K that the MWC can handle is quickly limited. In other words, for a given sparsity level K, the required number of branches increases if the mixing codes are not able to gather as much information as possible about the input signal in one measure. For Gaussian matrices, [7] shows that:

$$M \geq 2\rho K \log\left(\frac{N}{4K}\right), \tag{1}$$

where ρ depends on the code. Several solutions to overcome this limitation are mentioned in the literature, including serialized [8] or collapsed architectures [2].

In this context circulant matrices $\mathbf{C}$ arose interest regarding codes as they are also easy to generate and exist for every $\mathbf{M}$. As represented in (2) they can be defined by a shift of the N elements of the first branch's code $\mathbf{c}$ in the time domain $p_1(t)$ or by the diagonal $\sigma_{k\in\{1,\dots,N\}}$ in the frequency domain [9]:

$$\mathbf{C} = \begin{pmatrix} \overbrace{c_N \quad c_{N-1} \quad \dots \quad c_1}^{\text{temporal code in the first branch}} \\ c_1 \quad c_N \quad \dots \quad c_2 \\ \ddots \quad \ddots \quad \ddots \quad \vdots \\ c_{N-1} \quad c_{N-2} \quad \dots \quad c_N \end{pmatrix} = \mathbf{F}^{-1}\begin{pmatrix} \sigma_1 & 0 & 0 \\ 0 & \ddots & 0 \\ 0 & 0 & \sigma_N \end{pmatrix}\mathbf{F}, \tag{2}$$

where $\mathbf{F}$ is the Discrete Fourier Transform (DFT) matrix. The code $\mathbf{c}$ is then the inverse DFT (IDFT) of the sequence $\boldsymbol{\sigma}$ [10].

The authors in [4] compared random phase circulant matrices to random matrices for signal sparse in usual bases and a selection of M rows among N that is random or deterministic. They found no significant differences with usual sparse signals thus suggesting less randomness would suffice as well. Furthermore, the authors in [10] point out that randomly sampled deterministic sensing matrices generated from the inverse DFT of an unimodular sequence $\boldsymbol{\sigma}$ with perfect (or nearly perfect in a certain extent) autocorrelation guarantee, for signals sparse in time or frequency, better recovery than random filters, which target no specific sparsity domain. Universality guarantees are a common target in compressive sensing but this proves that there might be better options if we have knowledge of the sparsity domain.

One instance of such unimodular perfect codes are Zadoff-Chu codes. The IDFT of a Zadoff-Chu code with prime length is also a Zadoff-Chu code so both temporal and frequency definition would lead to the same matrice structure, which verifies the hypothesis in [10]. Zadoff-Chu sequences are complex-valued and constant envelope codes known in communications for synchronization in Long-Term Evolution (LTE) mobile communications systems due to their perfect cyclic autocorrelation function. They are defined by:

$$\begin{aligned} ZC_R[k] &= e^{-j\pi Rk(k-1)/N}, \\ &\text{for } k = \{1,\dots,N\}, R \text{ prime to } N \end{aligned} \tag{3}$$

As they have constant amplitude but varying phase, they simultaneously preserve the Power Spectral Density and create diversity in the projection. The architecture proposed in [11] and [12] uses randomly sampled complex circulant Zadoff-Chu codes. The study showed one promising simulation result ([11], Fig. 4.6), however it lacks a detailled high level metric analysis. They only argue that the RIP criterion (see Sect. III) of the sensing matrix will be the same as that from the selection matrix operator.

As a last remark, we want to point out that if we respect a simple symmetry condition [13] on the elements $\sigma_{k\in\{1,\dots,N\}}$ of a circulant matrix, we can generate a real circulant matrix which is of main interest compared to [6]:

$$\begin{array}{ll} k = \{1; \frac{N}{2}+1\} & \sigma_k = \pm 1 \text{with equ. prop.} \\ 2 \leq k < \frac{N}{2}+1 & \sigma_k = e^{j\phi_k} \\ \frac{N}{2}+2 < k \leq N & \sigma_k = \sigma^*_{N-k+2} \\ \text{for even N} & \end{array} \tag{4}$$

Those real circulant matrices can be viewed as a specific case of the random convolution introduced by [13] where phases are supposed to be uniformly distributed.

Based on previous elements, we propose a slightly new, real, sensing matrix. This real circulant matrix is obtained as the inverse DFT of a diagonal matrix created by the symmetry on a Zadoff-Chu sequence (noted "ZC circ real"), as pictured in (5):

$$\mathbf{C} = \mathbf{F}^{-1}\begin{pmatrix} 1 & 0 & 0 & 0 \\ 0 & ZC_R[2] & 0 & 0 \\ 0 & \ddots & \ddots & 0 \\ 0 & 0 & 0 & ZC^*_R[2] \end{pmatrix}\mathbf{F} \tag{5}$$

C. Objectives

In this paper we carried out a detailled study on the choice of optimal codes for the MWC based on multiple criteria, which permits to justify the use of circulant Zadoff-Chu codes. First, on the perspective to limit the number of branches and to simplify the hardware we need to collect as much information as possible. This is why we will focus on the coherence metric regarding various codes and selectors in Sect. II-A. Second, our goal is to guarantee a solution resilient to noise. To this end we will yield in Sect. III an estimation of isometric properties, with both a benchmark for Expected RIP (ExRIP) and an empirical estimation. Last we will validate our insights in simulation in Sect. IV.

II. Coherence analysis on codes and selectors

A. Definition

The coherence μ [1] is the largest absolute Hermitian inner product between any two different normalized columns of a matrix $\mathbf{A} = \mathbf{R_T}.\boldsymbol{\Theta} = \mathbf{R_T}.\boldsymbol{\Phi}.\boldsymbol{\Psi}$ of size $M \times N$ where $\mathbf{R_T}$ is an operator selecting M rows within N, $\boldsymbol{\Phi}$ is the matrix describing the measurement process and $\boldsymbol{\Psi}$ is the $N \times N$ matrix describing the basis in which the signal is sparse:

ISBN 978-0-9928626-7-1 © EURASIP 2017

$$\mu(\mathbf{A}) = \max_{i \neq j} \left(\frac{| < \mathbf{A}_{.,i}, \mathbf{A}_{.,j} > |}{\|\mathbf{A}_{.,i}\| \, \|\mathbf{A}_{.,j}\|} \right), \tag{6}$$

where $\mathbf{A}_{.,i}$ is the i^{th} column of $\mathbf{A}$. $\mathbf{\Theta}$ is then the initial full square sensing matrix whereas $\mathbf{A}$ is the dimension reduced sensing matrix after row selection. The coherence captures the fact that each projection should be orthogonal or nearly orthogonal, such that each component of the measurements captures a unique set of information about the input, and the information gathered globally is maximised. The coherence should be as small as possible, with a lower bound given by the Welch bound [14].

B. Coherence of typical matrices

We aim at comparing the coherence of the matrices typically benchmarked in Compressive Sensing and more advanced techniques recently investigated in the literature (Zadoff-Chu circulant [11], Gold circulant [2]). It is shown in [2] that the MWC sensing matrix can be expressed as $\mathbf{\Theta} = \mathbf{C}.\tilde{\mathbf{F}}.\mathbf{D}$ where $\tilde{\mathbf{F}}$ is a reordered subset of $\mathbf{F}$ and $\mathbf{D}$ is a diagonal matrix accounting for the decay of the code's Fourier transform at high frequencies that can be ignored in the coherence computation, due to normalization. We would like to know how much performances are influenced by the row selection within the square sensing matrix. In [11] a random selector is important to prove geometric properties, whereas in [4] the selector choice does not globally influence the practical results. We therefore computed the coherence for various selection schemes and growing M on Fig. 2. Selecting the pattern with best coherence among 1000 patterns chosen uniformly at random is noted "stat", naively taking the first lines is noted "fl", taking regularly spaced lines is noted "sub".

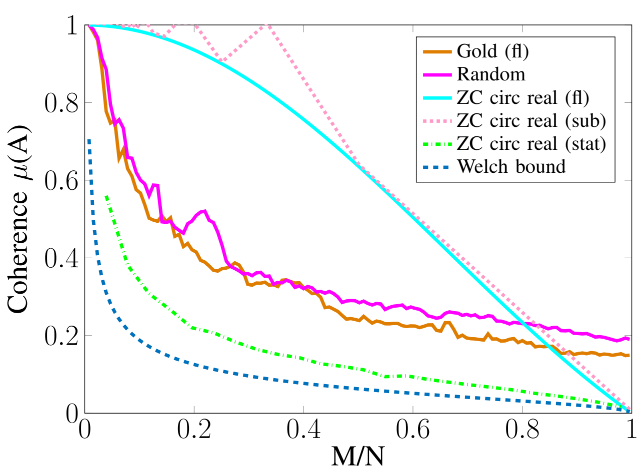

Fig. 2: Coherence comparison (N=255, R=1).

Random and Gold codes are outperformed by Zadoff-Chu circulant codes with "stat" selector. Fig. 2 also highlights that for Zadoff-Chu, the coherence depends highly on the selection of the codes. Naively taking the first lines for Zadoff-Chu would lead to a bad choice with poor coherence performances. For the sake of clarity not all curves are represented, but note that the coherence of Gold codes was similar with other selectors and complex circulant Zadoff-Chu codes coherence was the same as for real ones. Codes that have sufficiently low coherence must now prove their isometric properties.

III. Isometric properties

Isometric properties are a major pillar in the compressive sensing framework, but they are uncomputable. To get an intuition about the size and the behavior of the constants δ at stake in the preservation of norm and distance, a practical approach is chosen to achieve a reasonable estimation.

A. Definition

The **Restricted Isometry Property (RIP)** [1] highlights how much a vector can be deformed by the embedding in a smaller dimension: a matrix $\mathbf{\Phi}$ satisfies RIP with parameters (K, δ_K) if there exists a $\delta_K \in [0, 1]$ such that:

$$(1 - \delta_k) \|\mathbf{x}\|^2 \leq \|\mathbf{\Phi x}\|^2 \leq (1 + \delta_k) \|\mathbf{x}\|_2^2 \tag{7}$$

for all K-sparse vectors $\mathbf{x} \in \mathbb{R}^N$.
The **Johnson-Lindenstrauss Lemma (JLL)** [15] on the other hand guarantees the conservation of the pairwise distance during a dimensionality reduction and thus it is perhaps more adapted to partial restitution methods. Based on it, we can say that a matrix $\mathbf{\Phi}$ satisfies the JLL property with parameters (Q, K, δ_K) if there exists a $\delta_K \in [0, 1]$ such that:

$$(1 - \delta_k) \|\mathbf{u} - \mathbf{v}\|_2^2 \leq \|\mathbf{\Phi u} - \mathbf{\Phi v}\|_2^2 \leq (1 + \delta_k) \|\mathbf{u} - \mathbf{v}\|_2^2 \tag{8}$$

for all $\mathbf{u}$,$\mathbf{v}$ elements of a set of Q K-sparse vectors $\in \mathbb{R}^N$.

B. Empirical RIP and JLL

Empirical RIP and JLL constants are computed through statistical estimation. Such simulations are known to miss specific pathological cases [16] and be overoptimistic however we could expect that the maximum δ encountered in practice will almost always be close to the maximum δ_{N_v} estimated. For RIP we generated 10^8 test vectors, subdivided in $N_s = 1000$ subsets of $N_v = 10000$ vectors. Each vector of length 127 has $K = 6$ non-zero values, uniformly distributed on the support and with values uniformly distributed on $[-0, 5; 0, 5]$. We then projected them with a sensing matrix of dimension 50×127 to study the variations of the norm of vectors $\mathbf{x}$ through projection. For JLL, we similarly generated $N_s = 1000$ subsets of $N_v = 200$ vectors (19900 distances) to study the variations of the norm of distances between $\mathbf{u}$ and $\mathbf{v}$ through projection. To get an estimation of the isometry deviation likely encountered in practice, we established histograms of deltas for the subsets N_s, in Fig. 3 for RIP and Fig. 4 for JLL. We also reported the average $E_{N_s}(\delta_{N_v})$ and standard deviation $\sigma_{N_s}(\delta_{N_v})$ of δ between the different subsets.

The standard deviation being very small, the methodology is validated. Fig. 3 shows that RIP-δ is nearly 1.5 times smaller for sensing matrices based on real circulant Zadoff-Chu codes than Gold and Random codes (0.27 instead of 0.36 and 0.39). Fig. 4 shows that JLL-δ is more than 1.5 smaller for sensing matrices based on Zadoff-Chu circulant codes than Random

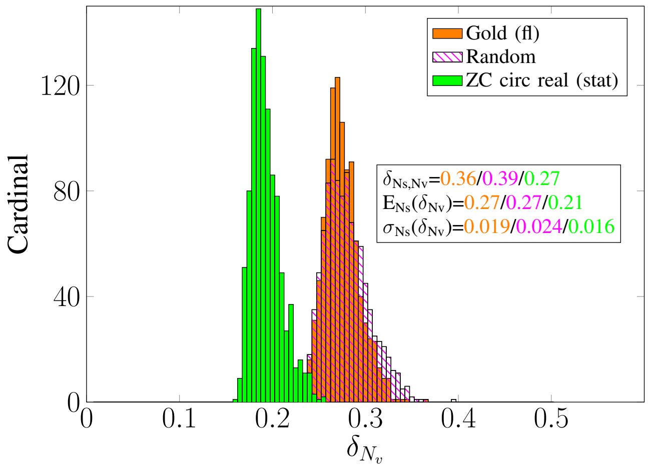

Fig. 3: Histogram of RIP-delta estimation (1000.10000, K=10).

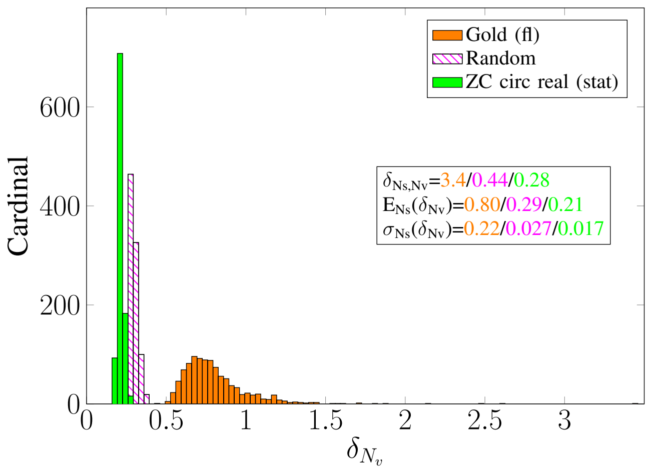

Fig. 4: Histogram of JLL-delta estimation (1000.200, K=10).

codes and more than 12 times smaller than Gold codes (0.28 instead of 0.44 and 3.4). This means we can reasonably rely on a small RIP and JLL constant for circulant Zadoff-Chu matrices.

C. Expected RIP (ExRIP)

The Expected RIP (ExRIP) criterion introduced by [17] gives the probability P that a matrix satisfies the RIP assuming a uniform distribution of the support and random distribution of non-zero values. It is easily computable based on three correlation criteria α, β and γ defined in [17]. To the best of the author's knowledge ExRIP guarantees are only established for real codes. Table I shows a comparison of ExRIP probability P that we have performed for various codes ("Ours", our results), benchmarked with results of [17]. Parameters of [17] are more detailled in the corresponding technical report [18].

It appears that circulant codes based on Zadoff-Chu sequences perform better than the other analyzed codes and that the statistical selector is slightly more effective. This can be related to their known good correlation properties.

TABLE I: ExRIP ($M = 511$, $K = 24$, $\delta_{2K} = \sqrt{2} - 1$)

Code		ZC(fl)	ZC(stat)	Random	Gold(fl)	Hadamard
P	Ours	0.9498	0.9511	0.927	0.9405	0
	[17]	–	–	0.927	0.939	0

IV. Platform validation

Isometric properties are linked to measurement noise resilience [19]. We want to confirm our previous results in numerical simulation and infer that codes with good isometric properties are indeed robust to noise. All simulations are based on a MATLAB platform inspired by [2] and available upon request. Parameters choices are $N = 127$, $f_s = f_p$ and Orthogonal Matching Pursuit (OMP) [20] as recovery algorithm. The input multiband signal is given by:

$$x(t) = \sum_{i=1}^{K/2} \sqrt{B}\, \text{sinc}(B(t - \tau_i)) \cos(2\pi f_i(t - \tau_i)), \qquad (9)$$

where $K = 6$, $B = 78\text{MHz}$, $f_{max} = 5\text{GHz}$, $\tau_i = \{0.4, 0.6, 0.8\}T_{acq}$, $T_{acq} = N/f_s$ and f_i are chosen uniformly at random.

An accurracy graph showing the percentage of support fully recovered with respect to the compression rate M/N is represented on Fig. 5 for both a noisy (10 dB Input Signal to Noise Ratio (ISNR)[21]) and a noiseless environment.

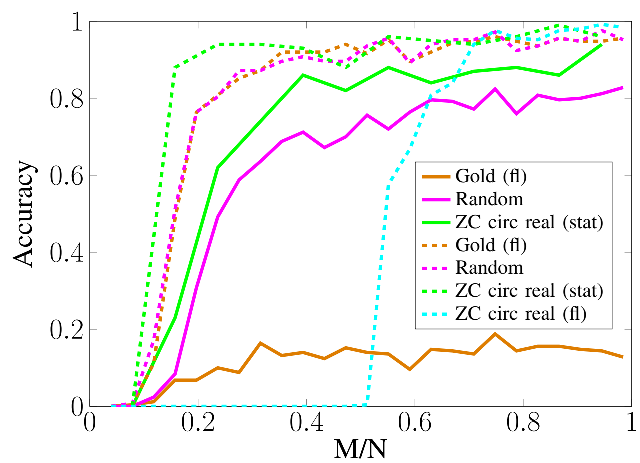

Fig. 5: Accuracy of the MWC with growing compression rate (K=6, 200 trials, OMP reconstruction algorithm), solid:10 dB ISNR, dashed: noiseless.

In the noiseless setting (dashed), Gold, circulant Zadoff-Chu with statistical selection and Random Bernoulli codes show similar good performances. It is striking that for Zadoff-Chu circulant codes, the success rate increases at small compression rate ($M/N > 0.05$) for statistical selection and at high compression ratio ($M/N > 0.5$) for first lines selection but that it reaches the same final performance. In fact this confirms that the required number of measurements is affected by coherence properties, which for Zadoff-Chu are dependent on the selector (and a naive selector is a bad choice as

ISBN 978-0-9928626-7-1 © EURASIP 2017

seen in Sect. IV). In the noisy context however, Gold codes performances collapse (at $M/N = 0.5$, 70% loss) whereas Zadoff-Chu codes degrade less (10% loss) than random codes (20% loss). Performances in a noisy context fit therefore our analysis of isometric properties: Zadoff-Chu circulant codes are indeed more resilient to noise than other analyzed codes. Note that complex Zadoff-Chu circulant codes, which are not shown for sake of curve's readibility, performed almost identically to the real version.

V. Conclusion

In conclusion this paper proposed a methodology for the evaluation of codes used in the MWC sensing matrix. Usual binary codes (Gold and Bernoulli) and more recent proposals have been benchmarked. We showed that real circulant codes based on Zadoff-Chu sequences are promising due to several reasons: first, they may be implemented with the storage of a N-length real code based on Zadoff-Chu sequences and of an arbitrary fixed M-length pattern selected randomly out of N time shifts. Second, they have good coherence, thus requiring an almost minimal number of branches and handling bad sparsity. More importantly they have excellent isometric properties, especially JLL which implies robustness against noise, in contrast to Gold codes. In addition, noise resilience of circulant codes based on Zadoff-Chu sequences has been verified by simulation means. Conceptually this solution can be seen as an implementation-friendly variation of the random convolution. Since isometric properties are also useful for classification purposes, perspectives would be to extend the analysis to signal classification.

References

[1] E. J. Candes *et al.*, "Compressive Sampling," *Proceedings of the International Congress of Mathematicians*, 2006.

[2] M. Mishali and Y. C. Eldar, "From Theory to Practice: Sub-Nyquist Sampling of Sparse Wideband Analog Signals," *IEEE Journal of Selected Topics in Signal Processing*, vol. 4, pp. 375–391, Apr 2010.

[3] D. L. Donoho, "Compressed sensing," *IEEE Transactions on Information Theory*, vol. 52, no. 4, pp. 1289–1306, April 2006.

[4] W. Yin, S. Morgan, J. Yang, and Y. Zhang, "Practical Compressive Sensing with Toeplitz and Circulant Matrices," in *Visual Communications and Image Processing 2010*, vol. 7744, 2010.

[5] R. T. Yazicigil, T. Haque, M. R. Whalen, J. Yuan, J. Wright, and P. R. Kinget, "Wideband Rapid Interferer Detector Exploiting Compressed Sampling With a Quadrature Analog-to-Information Converter," *IEEE Journal of Solid-State Circuits*, vol. 50, no. 12, pp. 3047–3064, Dec 2015.

[6] H. W. L. Gan and H. Wang, "Deterministic Binary Sequences for Modulated Wideband Converter," in *Proceedings of the 10th International Conference on Sampling Theory and Applications*, 2013.

[7] T. Haque, R. T. Yazicigil, K. J. L. Pan, J. Wright, and P. R. Kinget, "Theory and Design of a Quadrature Analog-to-Information Converter for Energy-Efficient Wideband Spectrum Sensing," *IEEE Trans. on Circuits and Systems I: Regular Papers*, vol. 62, no. 2, pp. 527–535, Feb 2015.

[8] O. Taheri and S. A. Vorobyov, "Segmented Compressed Sampling for Analog-to-Information Conversion: Method and Performance Analysis," *IEEE Trans. on Signal Processing*, vol. 59, no. 2, pp. 554–572, Feb 2011.

[9] H. Rauhut, "Compressive Sensing and Structured Random Matrices," *Theoretical foundations and numerical methods for sparse recovery*, vol. 9, pp. 1–92, 2010.

[10] K. Li, L. Gan, and C. Ling, "Convolutional Compressed Sensing Using Deterministic Sequences," *IEEE Transactions on Signal Processing*, vol. 61, no. 3, pp. 740–752, Feb 2013.

[11] X. Yang, "Research on Compressed Sensing and its Applications in Wireless Communications," Thesis, Macquarie University, 2015.

[12] X. Yang, Y. J. Guo, Q. Cui, X. Tao, and X. Huang, "Random circulant orthogonal matrix based analog compressed sensing," in *2012 IEEE Global Communications Conference (GLOBECOM)*, Dec 2012, pp. 3605–3609.

[13] J. Romberg, "Compressive Sensing by Random Convolution," *SIAM Journal on Imaging Sciences*, vol. 2, no. 4, pp. 1098–1128, 2009.

[14] L. Welch, "Lower bounds on the maximum cross correlation of signals," *IEEE Trans. on Information Theory*, vol. 20, no. 3, pp. 397–399, 1974.

[15] R. Baraniuk, M. Davenport, R. DeVore, and M. Wakin, "A Simple Proof of the Restricted Isometry Property for Random Matrices," *Constructive Approximation*, vol. 28, no. 3, pp. 253–263, 2008.

[16] C. Dossal, G. Peyre, and J. Fadili, "A numerical exploration of compressed sampling recovery," *Linear Algebra and its Applications*, 2010.

[17] M. Mishali and Y. C. Eldar, "Expected Rip: Conditioning of The Modulated Wideband Converter," in *Information Theory Workshop, 2009. ITW 2009. IEEE*, Oct 2009, pp. 343–347.

[18] ——, "Conditioning of the modulated wideband converter," *CCIT Technion Report*, 2009.

[19] M. Davenport, "Random Observations on Random Observations: Sparse Signal Acquisition and Processing," Thesis, Rice University, 2010.

[20] J. A. Tropp and A. C. Gilbert, "Signal Recovery From Random Measurements Via Orthogonal Matching Pursuit," *IEEE Transactions on Information Theory*, vol. 53, no. 12, pp. 4655–4666, Dec 2007.

[21] M. A. Davenport, J. N. Laska, J. R. Treichler, and R. G. Baraniuk, "The Pros and Cons of Compressive Sensing for Wideband Signal Acquisition: Noise Folding versus Dynamic Range," *IEEE Trans. on Signal Processing*, vol. 60, no. 9, pp. 4628–4642, Sept 2012.

ISBN 978-0-9928626-7-1